

## Millimeter-wave rotational transitions and molecular constants of the diatomic molecule AgBr

K. P. R. Nair and J. Hoefl

*Institut für Molekülphysik der Freien Universität Berlin, Arnimallee 14,  
D-1000 Berlin 33, West Germany*

(Received 9 June 1986)

In the 280-GHz frequency region several rotational transitions of AgBr in four vibrational states ( $v=0,1,2,3$ ) have been observed. The analysis resulted in extended and independent sets of Dunham parameters  $Y_{01}$ ,  $Y_{11}$ ,  $Y_{21}$ ,  $Y_{02}$ , and  $Y_{03}$  of the four natural isotopic species  $^{107}\text{Ag}^{79}\text{Br}$ ,  $^{109}\text{Ag}^{79}\text{Br}$ ,  $^{107}\text{Ag}^{81}\text{Br}$ , and  $^{109}\text{Ag}^{81}\text{Br}$ . With these microwave data the constants  $\omega_e$  and  $\omega_e x_e$  were calculated. The parameters of the Dunham potential  $a_0$ ,  $a_1$ ,  $a_2$ ,  $a_3$ , and  $r_e$  are given.

## I. INTRODUCTION

Franck and Kuhn<sup>1</sup> established the existence of the AgBr monomer in the gas phase by observation of electronic transitions in the near-ultraviolet region. These studies of the absorption spectra were extended by Brice,<sup>2</sup> Metropolis and Beutler,<sup>3</sup> and Barrow and Mulcahy<sup>4</sup> with the detection of additional electronic transitions. The evaluation of band heads resulted in vibrational constants of the four isotopic species which have almost identical natural abundances. But an analysis of the complex rotational structure of electronic transitions has not yet been reported. Krisher and Norris<sup>5</sup> studied some pure rotational transitions in the microwave region between 11 and 32 GHz. Two of these transitions showed a doublet structure indicating the influence of the nuclear quadrupole interaction between the nuclei of the Br atoms and the gradient of the electric field along the molecular axis. We studied the hyperfine structure of the rotational transition  $J=3\leftarrow 2$  at 12 GHz in more detail.<sup>6</sup> The detection of the weaker hyperfine-structure components with enhanced sensitivity and resolution resulted in coupling constants with an accuracy improved by more than a factor of 100. In our earlier studies we restricted these observations to  $^{107}\text{Ag}^{79}\text{Br}$  and  $^{109}\text{Ag}^{79}\text{Br}$  only, because the ratio of the nuclear quadrupole moments of  $^{79}\text{Br}$  and  $^{81}\text{Br}$  was determined precisely by other methods. But we extended the measurements to the first excited vibrational state. By evaluation of the Stark-effect frequency splittings of selected hyperfine components of both isotopic species we determined the electric dipole moment of AgBr in its electronic and vibrational ground state.<sup>7</sup>

The investigations in the microwave region involved only rotational transitions at lower frequencies with rotational quantum numbers  $J=8$  in maximum. However, studies of rotational transitions at higher frequencies involving large  $J$  numbers allow the determination of more rotational parameters with improved accuracy. Often the knowledge of these parameters is needed for assignment and interpretation of the complex structure of electronic transitions of heavier molecules like AgBr. In many cases there is a strong correlation between the data sets of both electronic states involved. Therefore the accuracy of the

data for both states is reduced substantially when there is high correlation. Precise microwave measurements can remove this correlation by independent determination of the molecular parameters in the ground state of the molecule.

In addition, rotational transitions with large quantum numbers  $J$  involve remarkable frequency shifts, due to centrifugal distortion,<sup>8</sup> described by the term  $4Y_{02}(J+1)^3$ , though  $Y_{02}$  is typically only of the order  $10^{-6}Y_{01}$ . The parameter  $Y_{02}$  is related to the vibrational constant  $\omega_e$ . In a similar way, an independent determination of  $\omega_e x_e$  with microwave data is possible.

As mentioned above the determination of the vibrational constants of AgBr from band spectra<sup>2</sup> was handicapped because of the lack of rotational analysis of the observed electronic transition. Hence, systematic errors in the analysis could not be excluded. Therefore, an independent determination of the vibrational parameters was one of the main subjects of this work.

We report here the results of measurements in the 280-GHz frequency region on all isotopic species of AgBr in vibrational states up to  $v=3$ . The rotational transitions observed involve quantum number  $J=76$  in maximum.

## II. EXPERIMENTAL

The monomers of AgBr were produced by vaporizing crystalline powder of commercial silver bromide in an alumina crucible with a Broida-type oven<sup>9</sup> at temperatures around 500°C. With typical evaporation rates of 5 g per hour we had run times of three hours maximum. The transport of the molecules into the absorption region between two horns of the free space cell was supported by a steady stream of argon carrier gas. A block diagram of the microwave spectrometer is given in Fig. 1. The absorption cell (length 1 m, inner diameter 0.15 m) built by one cross and one T component of borosilicate glass (Duran, Schott) was operated at room temperature. With original polytetrafluorethylene (PTFE) gaskets prepared with silicon vacuum grease we obtained a total pressure of  $10^{-5}$  mbar after careful outgassing. During the measurements the cell was continuously pumped with a booster pump (9 B 3, Edwards) coupled to a mechanical pump

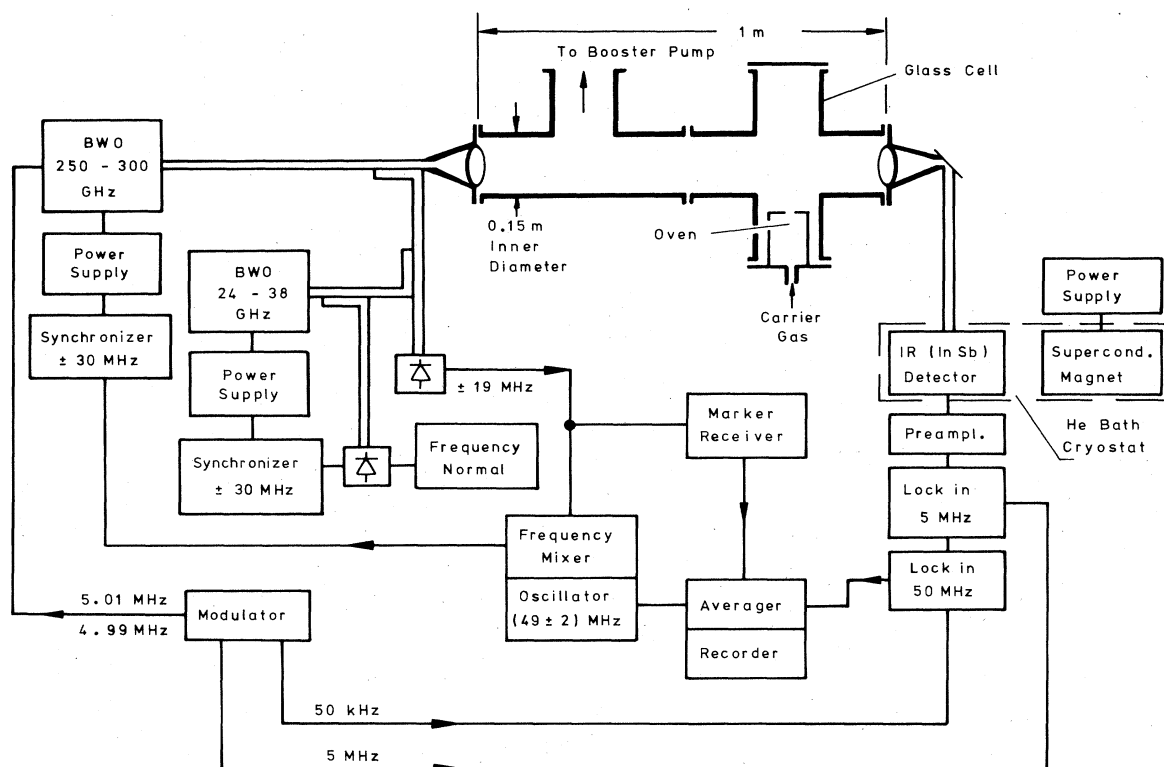


FIG. 1. Block diagram of the microwave spectrometer.

(T 1030, Alcatel). A liquid-nitrogen trap between cell and booster pump was used to prevent corrosion of the pump system. The installation of an additional trap between booster and mechanical pump was essential for chemical protection of the mechanical pump.

In microwave spectroscopy the total pressure in the absorption region must be lower than in optical spectroscopy in order to prevent a reduction of resolution by pressure broadening. Figure 1 shows that we used a saturation modulation scheme described by Törning<sup>10</sup> to detect the small microwave absorption signals. For this technique the microwave power must be high enough so that the nonlinearity of the absorption becomes noticeable. However, this condition sets an upper limit to the total pressure in the absorption region as well. In this experiment with AgBr we found the optimum of the argon pressure in the absorption cell at  $5 \times 10^{-3}$  mbar. Inside the oven system the argon pressure is substantially higher.

The measurements were carried out with a backward wave oscillator BWO [CO 10 B, Thomson-CSF (Laboratoire Central de Recherches, Thomson-CSF, Orsay, France)] phase synchronized in two steps to a frequency standard (01500 and FSS 1500, Schlumberger). In the first step the 300-GHz BWO was synchronized to a 30-GHz BWO (F 4034 B, Thomson-CSF). Both synchronizers (FDS 30, Schomandl) receive difference frequencies of 30 MHz. For frequency sweep of the phase-synchronized 300-GHz source a 19-MHz difference signal with the 8th harmonic of the second BWO is mixed with the frequency

of a 49-MHz oscillator tunable by the ramp voltage of an averager system (1020 A, Nicolet). In this manner the 300-GHz source can be tuned electronically around  $\pm 2$  MHz in the phase-synchronized state. For observation of larger frequency regions a motor drive at the frequency standard can be used to sweep the phase-locked microwave source. The microwave was coupled through the absorption region by two horn antennas fixed to the ends of the glass cell and equipped with PTFE lenses improving the microwave transmission of the absorption cell.

The microwave signals were detected by an InSb infrared detector (IRD-4, Advanced Kinetics) housed in a helium-bath cryostat. The bolometer crystal was operated at temperatures around 1.5 K in a magnetic field of  $12\,000 \text{ A m}^{-1}$  produced by a surrounding superconducting coil. Two separate vacuum pump systems served for thermal vacuum isolation in the cryostat and pumping helium gas to obtain temperatures below 4.2 K.

The full linewidths of 300 kHz observed in the 280-GHz region were of the same magnitude as in our former measurements at 12 GHz.<sup>6,7</sup> Therefore the precision of line frequency measurements are believed to be accurate to at least  $\pm 30$  kHz. To minimize systematic errors due to instrumental distortions all frequency measurements were taken with forward and reverse frequency sweeps at both frequency sidebands of the 300-GHz BWO produced by the modulation technique.<sup>10</sup> The maximum signal-to-noise ratio was 30 using a time constant of 1 s at 6 dB/octave.

### III. ANALYSIS AND RESULTS

The frequency of the transitions measured in the 280 GHz region are given in Table I. The frequencies of the  $J=3\leftarrow 2$  transition of  $^{107}\text{Ag}^{79}\text{Br}$  and  $^{109}\text{Ag}^{79}\text{Br}$  at 12 GHz are included and describe the hypothetical unsplit transitions obtained by analysis of the hyperfine structure.<sup>6</sup> The frequencies of transitions measured by Krisher and Norris<sup>5</sup> were not included in the analysis because of the much smaller precision. The statistical weight of these measurements would be too small in an overall fit.

If the interaction between nuclei and molecular rotation may be neglected the energy eigenvalues of the vibrating rotator can be represented by Dunham's solution of the time-independent Schrödinger equation<sup>11</sup> where the potential function is developed in the form

$$U(\xi) = cha_0\xi^2(1 + a_1\xi + a_2\xi^2 + a_3\xi^3 + \dots) \\ + hB_eJ(J+1)(1 - 2\xi + 3\xi^2 - \dots),$$

with  $\xi = (r - r_e)/r_e$ ,  $B_e = h/8\pi^2\mu r_e^2$ , and  $r_e$  is the equilibrium distance between the nuclei,  $\mu$  the reduced mass of the molecule,  $h$  Planck's constant, and  $c$  the velocity of light.

The frequencies of rotational electric dipole transitions follow the relation<sup>8</sup>

$$\nu_{v,J+1-v,J} = 2[Y_{01} + Y_{11}(v+1/2) + Y_{21}(v+1/2)^2 \\ + Y_{31}(v+1/2)^3 + \dots](J+1) \\ + 4[Y_{02} + Y_{12}(v+1/2) + \dots](J+1)^3 \\ + Y_{03}(J+1)^3[(J+2)^3 - J^3] + \dots$$

Some Dunham parameters  $Y_{kl}$  are related to more familiar spectroscopic constants like

$$Y_{01} \approx B_e, \quad Y_{02} \approx -D_e, \quad Y_{03} \approx H_e,$$

$$Y_{11} \approx -\alpha_e, \quad Y_{12} \approx -\beta_e, \quad Y_{21} \approx \gamma_e.$$

The parameters  $Y_{10}$  and  $Y_{20}$  cannot be determined directly by observation of pure rotational transitions. However, they may be calculated with sufficient accuracy from  $Y_{kl}$  measured in rotational transitions by the following relations:

$$\omega_e \approx Y_{10} = 2(Y_{01}^3 / -Y_{02})^{1/2},$$

$$\omega_e x_e \approx -Y_{20} = -3Y_{01}(a_2 - 5a_1^2/4)/2,$$

where  $a_1$  and  $a_2$  are constants of the Dunham potential function. The first four constants in terms of the energy coefficients  $Y_{kl}$  are

$$a_0 = Y_{01}^2 / -Y_{02},$$

$$a_1 = Y_{11}/3(-Y_{02}Y_{01})^{1/2} - 1,$$

$$a_2 = \frac{1}{6}Y_{12}(Y_{01}/-Y_{02})^{1/2} + 9a_1(2+a_1)/8 + \frac{19}{8},$$

$$a_3 = -2Y_{21}/15Y_{02} + a_2(3+13a_1)/5 \\ - a_1[4+3a_1(1+a_1)]/2 - 1.$$

The results for the Dunham parameters of the four natural isotopic species of AgBr are given in Table II. Table III shows the potential constants. By a first least-squares fit of the line frequencies we got preliminary

TABLE I. Observed rotational transitions  $J+1\leftarrow J$  and frequencies in MHz of AgBr.

$J$	$v$	$^{107}\text{Ag}^{79}\text{Br}$		$^{109}\text{Ag}^{79}\text{Br}$		$^{107}\text{Ag}^{81}\text{Br}$		$^{109}\text{Ag}^{81}\text{Br}$	
		Obs.	Obs. minus Calc.	Obs.	Obs. minus Calc.	Obs.	Obs. minus Calc.	Obs.	Obs. minus Calc.
2 <sup>a</sup>	0	11 640.579	-0.009	11 549.887	-0.004				
	1	11 598.192	0.008	11 507.995	0.014				
70	0	274 743.628	-0.004						
	1	273 740.079	0.011						
71	0	278 591.608	-0.015	276 427.127	-0.016	274 648.705	-0.011		
	1	277 573.931	0.006	275 421.323	0.012	273 652.655	0.037		
	2	276 557.819	-0.010						
	3	275 543.318	-0.016						
72	0	282 438.725	0.020	280 244.510	-0.002	278 441.684	0.010	276 247.274	0.004
	1	281 406.866	-0.007	279 224.720	0.009	277 431.718	-0.023	275 249.332	-0.033
	2	280 376.677	0.013	278 206.508	-0.003	276 423.362	-0.008		
	3	279 348.102	0.023						
73	0	286 284.862	-0.005	284 060.978	0.004	282 233.729	-0.008	280 009.572	-0.037
	1	285 238.900	0.001	283 027.182	-0.021	281 209.942	-0.027	278 997.958	-0.009
	2	284 194.563	-0.015	281 995.059	0.003	280 187.787	0.002	277 987.916	0.018
	3	283 151.900	-0.003						
74	0			287 876.529	0.013	286 024.900	0.008	283 771.053	-0.001
	1			286 828.775	-0.000	284 987.304	0.014	282 745.713	-0.029
	2					283 951.299	0.006	281 722.006	-0.017
75	0							287 531.628	0.034
								286 492.617	0.006

<sup>a</sup>Frequencies of the hypothetical unsplit transitions from analysis of hyperfine structure (Ref. 6).

TABLE II. Molecular constants of AgBr. Values in parentheses are one standard deviation.

	<sup>107</sup> Ag <sup>79</sup> Br	<sup>109</sup> Ag <sup>79</sup> Br	<sup>107</sup> Ag <sup>81</sup> Br	<sup>109</sup> Ag <sup>81</sup> Br
$Y_{01}$ (MHz)	1943.6453 (8)	1928.4876 (8)	1916.0328 (16)	1900.8794 (23)
$Y_{11}$ (MHz)	-7.078 47 (10)	-6.995 91 (17)	-6.928 04 (28)	-6.846 04 (38)
$Y_{21}$ (kHz)	5.56 (3)	5.49 (6)	5.35 (9)	5.31 (13)
$Y_{02}$ (kHz)	-0.524 65 (8)	-0.516 43 (8)	-0.509 61 (14)	-0.501 91 (20)
$Y_{03}$ (mHz) <sup>a</sup>	-0.047 66 (3)	-0.046 57 (3)	-0.045 68 (6)	-0.044 57 (10)
$Y_{10} \approx \omega_e$ (cm <sup>-1</sup> ) <sup>b</sup>	249.574 (19)	248.616 (19)	247.852 (34)	246.790 (49)
$Y_{20} \approx \omega_e x_e$ (cm <sup>-1</sup> ) <sup>b</sup>	0.635 (5)	0.630 (5)	0.626 (9)	0.621 (12)

<sup>a</sup>Calculated and used as fixed parameter in the final fit.

<sup>b</sup>Calculated with  $c_0 = [2.997\,924\,58(1)] \times 10^8 \text{ ms}^{-1}$ .

values of  $Y_{01}$ ,  $Y_{11}$ ,  $Y_{21}$ , and  $Y_{02}$ .  $Y_{03}$  was obtained by the relation

$$Y_{03} = Y_{02}^2(a_1 + 3)/Y_{01}$$

with higher accuracy than from a direct fit. Fits including  $Y_{31}$  and  $Y_{12}$  showed no relevance to these parameters considering their statistical errors. In the final fit  $Y_{03}$  was used as fixed parameter.

The deviations between the observed frequencies and the frequencies calculated with the final values of  $Y_{01}$ ,  $Y_{11}$ ,  $Y_{21}$ ,  $Y_{02}$ , and  $Y_{03}$  from Table II are given in Table I. They do not exceed the experimental errors considerably. The errors given in Tables II and III are one standard deviation. In the cases of the potential constants  $a_2$  and  $a_3$  in Table III the errors include the contribution of  $Y_{12}$  neglected in the final fit. The Dunham correction<sup>8</sup>

$$C_{01}(B_e/\omega_e)^2 = \frac{Y_{01} - B_e}{B_e}$$

with

$$C_{01} = (Y_{21}/-Y_{02}) - 8a_1 - 6a_1^2 - 6a_1^3 + 8a_1a_2$$

describes the relative difference between  $Y_{01}$  and the rotational constant

$$B_e = h/8\pi^2\mu r_e^2.$$

For all isotopic species of AgBr we got

$$\frac{Y_{01} - B_e}{B_e} = -2.6 \times 10^{-7}.$$

This is only one-half or less of one standard error of  $Y_{01}$ . Therefore, we calculated the internuclear distance  $r_e$  directly by the relation

$$r_e = [505\,390.98(350)/\mu Y_{01}]^{1/2},$$

where the  $Y_{01}$  value is to be given in MHz. The reduced molecular masses given in atomic mass units in Table III were calculated with atomic masses collected by Wapstra and Bos.<sup>12</sup> The conversion factor was determined with the natural constants given by Cohen and Taylor.<sup>13</sup>

The measured parameters  $Y_{kl}$  follow the general mass relations between two isotopic species of a molecule<sup>8</sup>

$$\frac{Y_{kl}(1)}{Y_{kl}(2)} = \left[ \frac{\mu^{(2)}}{\mu^{(1)}} \right]^{(k+2l)/2}$$

within the experimental errors (one standard deviation).  $\mu^{(1)}$  and  $\mu^{(2)}$  stand for the reduced masses of the two isotopic species, so there is no indication of a breakdown of the Born-Oppenheimer approximation. This fact is also demonstrated by the agreement of the potential constants  $a_0$ ,  $a_1$ ,  $a_2$ ,  $a_3$ , and  $r_e$  of the four isotopic species within the given errors.

In Table IV the results for the rotational parameters of <sup>107</sup>Ag<sup>79</sup>Br are given in comparison with the results of pre-

TABLE III. Potential constants and reduced masses  $\mu$  of AgBr. Values in parentheses are one standard deviation.

	<sup>107</sup> Ag <sup>79</sup> Br	<sup>109</sup> Ag <sup>79</sup> Br	<sup>107</sup> Ag <sup>81</sup> Br	<sup>109</sup> Ag <sup>81</sup> Br
$a_0$ (cm <sup>-1</sup> ) <sup>a</sup>	240 184 (37)	240 216 (37)	240 296 (66)	240 139 (96)
$a_1$	-3.336 55 (18)	-3.336 73 (18)	-3.337 04 (32)	-3.336 29 (46)
$a_2$	7.39 (5)	7.39 (5)	7.39 (9)	7.39 (13)
$a_3$	-13.6 (4)	-13.6 (4)	-13.6 (7)	-13.6 (10)
$r_e$ (10 <sup>-10</sup> m) <sup>b</sup>	2.393 135 6 (8 3) <sup>c</sup> (5)	2.393 136 3 (8 3) <sup>c</sup> (5)	2.393 137 3 (8 3) <sup>c</sup> (1 0)	2.393 135 2 (8 3) <sup>c</sup> (1 5)
$\mu^d$	45.402 090 4	45.758 921 2	46.056 329 9	46.423 560 2

<sup>a</sup>Calculated with  $c_0 = [2.997\,924\,58(1)] \times 10^8 \text{ ms}^{-1}$ .

<sup>b</sup> $r_e = [505\,390.98(350)/\mu Y_{01}]^{1/2}$  with  $r_e$  in 10<sup>-10</sup> m,  $\mu$  in amu, and  $Y_{01}$  in MHz.

<sup>c</sup>Systematic error from the uncertainty of the natural constants (see also footnote b).

<sup>d</sup>Calculated with atomic masses from Ref. 10.

TABLE IV. Comparison of some constants of  $^{107}\text{Ag}^{79}\text{Br}$  with results of former works.

	This work	Previous works
$Y_{01}$ (MHz)	1943.6453 (8)	1943.6420 (50) <sup>a</sup>
$Y_{11}$ (MHz)	-7.078 47 (10)	-7.0745 (70) <sup>a</sup>
$Y_{21}$ (MHz)	5.56 (3)	5.02 (45) <sup>b</sup>
$Y_{02}$ (kHz)	-0.524 65 (8)	-0.53 (13) <sup>b</sup>
$Y_{03}$ (mHz)	-0.047 66 (3)	

<sup>a</sup>See Ref. 6.<sup>b</sup>See Ref. 5.

vious works.<sup>5,6</sup> This example gives an idea of the improvements available by spectroscopy in the 1-mm wavelength region. Table V compares the results for the vibrational parameters of  $^{109}\text{Ag}^{81}\text{Br}$  with those from band spectra.<sup>2</sup> The discrepancies have to be discussed under consideration of the fact that Brice<sup>2</sup> could not resolve the ro-

TABLE V. Vibrational constants of  $^{109}\text{Ag}^{81}\text{Br}$  in comparison with results from a previous work.

	This work	Previous work <sup>a</sup>
$\omega_e$ ( $\text{cm}^{-1}$ )	246.790 (49)	247.72
$\omega_e x_e$ ( $\text{cm}^{-1}$ )	0.621 (12)	0.6795

<sup>a</sup>See Ref. 2.

tational structure of the observed electronic transition  $B-X$  sufficiently. The author gives no error limits, and the influence of possible systematic errors is not mentioned.

## ACKNOWLEDGMENT

This work has been performed under Sonderforschungsbereich 161 of the Deutsche Forschungsgemeinschaft.

<sup>1</sup>J. Franck and H. Kuhn, *Z. Phys.* **44**, 607 (1927).<sup>2</sup>B. A. Brice, *Phys. Rev.* **38**, 658 (1931).<sup>3</sup>M. Metropolis and H. Beutler, *Phys. Rev.* **55**, 1113 (1939).<sup>4</sup>R. F. Barrow and M. F. R. Mulcahy, *Nature (London)* **162**, 336 (1948).<sup>5</sup>L. C. Krisher and W. G. Norris, *J. Chem. Phys.* **44**, 974 (1966).<sup>6</sup>J. Hoelt, F. J. Lovas, E. Tiemann, and T. Törring, *Z. Naturforsch. Teil A* **26**, 240 (1971).<sup>7</sup>K. P. R. Nair and J. Hoelt, *Chem. Phys. Lett.* **102**, 438 (1983).<sup>8</sup>C. H. Townes and A. L. Schawlow, *Microwave Spectroscopy* (McGraw-Hill, New York, 1955). See also K. P. R. Nair,H.-U. Schütze-Pahlmann, and J. Hoelt, *Chem. Phys. Lett.* **70**, 585 (1980).<sup>9</sup>J. B. West, R. S. Bradford, J. D. Everrole, and C. W. Jones, *Rev. Sci. Instrum.* **46**, 164 (1975).<sup>10</sup>T. Törring, *J. Mol. Spectrosc.* **48**, 148 (1973).<sup>11</sup>J. L. Dunham, *Phys. Rev.* **41**, 721 (1932).<sup>12</sup>A. H. Wapstra and K. Bos, *At. Data. Nucl. Data Tables* **19**, 177 (1977).<sup>13</sup>E. R. Cohen and B. N. Taylor, *J. Phys. Chem. Ref. Data* **2**, 717 (1973).